*Int. J. Electrochem. Sci.*, 17 **(2022)** Article Number: 22047, doi: 10.20964/2022.04.42

International Journal of
ELECTROCHEMICAL
SCIENCE
www.electrochemsci.org

# Theoretical Analysis of Transient Responses of Amperometric Biosensor Based on the Phenol–Polyphenol Oxidase Model

*R. Joy Salomi*[1], *S. Vinolyn Sylvia*[1], *Marwan Abukhaled*[2], *Michael E.G. Lyons*[3], *L. Rajendran*[1,*]

[1] Department of Mathematics, Academy of Maritime Education and Training (AMET), India
[2] Department of Mathematics and Statistics, American University of Sharjah, Sharjah, UAE
[3] School of Chemistry & AMBER National Centre, University of Dublin, Trinity College Dublin, Dublin 2, Ireland
[*]E-mail: raj_sms@rediffmail.com

*Received:* 1 December 2021 / *Accepted:* 7 February 2022 / *Published:* 4 March 2022

An amperometric biosensor based on the phenol–polyphenol oxidase model for transient conditions is discussed. The model is based on the reaction-diffusion equation containing a nonlinear term related to the Michaelis-Menten kinetics of the enzymatic reaction. Modified homotopy perturbation and Akbari-Ganji methods are employed to solve the system of nonlinear differential equations. As a result, approximate analytical expressions for substrate and product concentrations are obtained. Closed-form analytic expressions for the corresponding current response, sensitivity of bioelectrode, and the amplification factor are also derived. A study on influence of the parameters on sensitivity has been presented. All derived analytical results are validated by comparing with numerical simulations.

**Keywords:** Mathematical modelling, Michaelis-Menten kinetics, bioelectrode, Laponite hydrogels, Homotopy perturbation method, Akbari-Ganji method

## 1. INTRODUCTION

An enzyme electrode is a small chemical transducer that integrates an electrochemical process with immobilized enzyme actions [1]. The enzyme electrodes find application in electrochemical immunoassays [2, 3], water pollutant detection [4, 5], and monitoring biological metabolites [6]. Substrate recycling greatly enhances the sensitivity of enzyme electrodes. Approaches to this kind of amplification include regeneration of the enzyme-substrate via a chemical reaction [7, 8] and enzymatic reaction that speeds up converting the first enzymatic step product back to the substrate [9, 10]. Here monitoring of co-product synthesis or co-substrate consumption induces transduction. This amplification can be achieved at the enzymatic step when the product is oxidized or reduced back to the substrate [11-13].

A theoretical study of enzyme electrodes is essential to understand the mechanism and kinetics of a biosensor. The insights gleaned from the theoretical models can be applied to optimize sensors, predict electrode response and sensors design. Desprez and Labbe [14] developed a kinetic model for the electroenzymatic processes involved at a PPO-rotating-disk bioelectrode that detects low catechol substrate concentrations. However, this model has its foundations on Bartlett and Whitaker's glucose sensor [15]. The prime importance of this model is that it can determine phenolic chemicals and catecholamine neurotransmitters in environmental and clinical investigation [16-19]. Using molecular dioxygen, PPO catalyzes orthodiphenol compound oxidation to orthoquinone [14]. The steady-state substrates and product concentrations for the first-order reactions ($[S_i] \leq K_i$ ) were reported by Coche-Guerente et al. [20]. The coupled time-independent nonlinear reaction-diffusion equations for the PPO system were solved analytically and numerically for all parameter values by Indira et al. [21]. However, a rigorous analytical expression for transient concentration and current for all parameter values is yet to be reported.

In this paper, the approximate analytical expressions for the substrate and product concentrations has been obtained using the homotopy perturbation method (HPM) and Akbari-Ganji method (AGM). In addition, more compact and closed general analytical expressions for sensitivity and amplification factors are also presented.

## 2. MATHEMATICAL FORMULATION OF THE PROBLEM

Coche-Guerente et al. presented a concise discussion and derivation of the dimensionless mass transport equation for amperometric biosensor [20]. The steps that lead to the electrode response are: (i) The assumption that the diffusion coefficients of phenol substrate $S_1$, catechol substrate $S_2$, and o-quinone product $P_2$ are equal in the bulk solution due to structural similarity. (ii) Diffusions of $S_1, S_2$, and $P_2$ are within the enzyme layer of thickness $L$ and with same diffusion coefficient $D_\mathrm{f}$ as well as same partition coefficient $\kappa$. (iii) The enzymatic reactions of substrates $S_1, S_2$, and the product $P_2$ follow Michaelis–Menten formalism in a homogeneous medium, i.e. $V_1 = \frac{k_1[E_\mathrm{T}][S_1]}{K_1+[S_1]}$ and $V_2 = \frac{k_2[E_\mathrm{T}][S_2]}{K_2+[S_2]}$, where $V_1$ and $V_2$ represent the enzymatic rate of o-quinone formation from phenol and catechol substrates, respectively. $[E_\mathrm{T}]$ represents the total concentration of active enzyme and $K_1, K_2, k_1$ and $k_2$ are the kinetic parameters. The electroenzymatic process (Figure 1) is as follows [20]:

At the solution (step C): $\mathrm{S_1 + O_2} \xrightarrow{\text{PPO}} \mathrm{P_2 + H_2O} \quad V_1$ (1)

At the electrode (step E): $\mathrm{P_2} + 2e^- + 2H^+ \underset{K_0}{\overset{K_\mathrm{f}}{\rightleftharpoons}} S_2 \quad E^\circ$ (2)

At the solution (step C'): $S_2 + \frac{1}{2}O_2 \xrightarrow{\text{PPO}} P_2 + \mathrm{H_2O} \quad V_2$ (3)

where $E^\circ$ is the standard potential of the $P_2/S_2$ redox system.

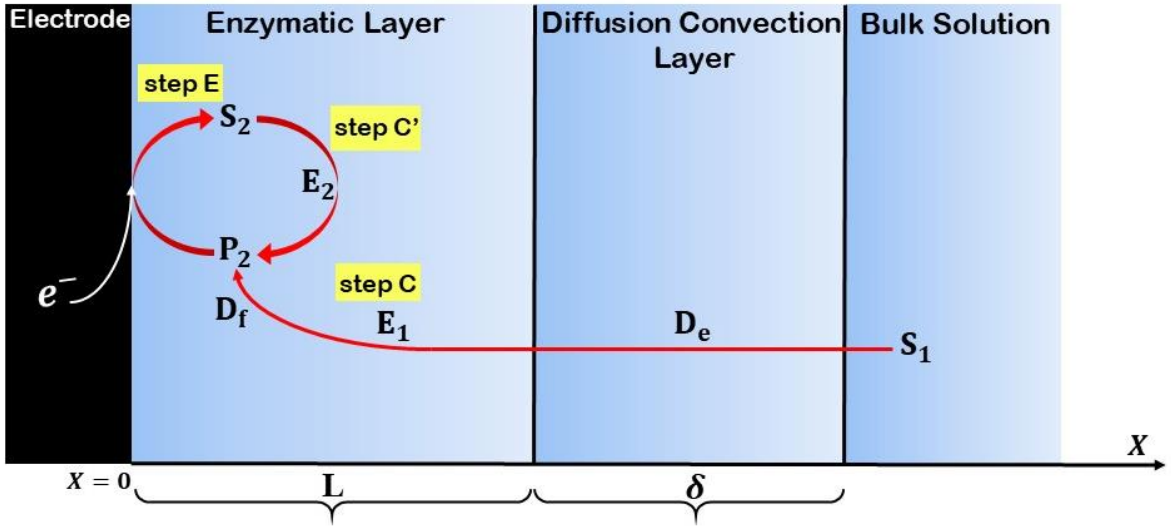


**Figure 1.** Illustration of the processes taking place at the rotating disk electrode (RDE) modified by a polyphenol oxidase (PPO) enzymatic layer and the principle of bioelectrode operation in the presence of phenol substrates $S_1$, $S_2$, and product $P_2$[20].

The transient system following Michaelis–Menten kinetics characterised by the substrates and product concentrations within the enzyme layer can be written as [20]:

$$\frac{1}{D_f}\frac{\partial[S_1](X,T)}{\partial T} = \frac{\partial^2[S_1](X,T)}{\partial X^2} - \frac{[S_1](X,T)}{\Lambda_1^2\left(1+\left(\frac{[S_1](X,T)}{K_1}\right)\right)} \quad (4)$$

$$\frac{1}{D_f}\frac{\partial[S_2](X,T)}{\partial T} = \frac{\partial^2[S_2](X,T)}{\partial X^2} - \frac{[S_2](X,T)}{\Lambda_2^2\left(1+\left(\frac{[S_2](X,T)}{K_2}\right)\right)} \quad (5)$$

$$\frac{1}{D_f}\frac{\partial[P_2](X,T)}{\partial T} = \frac{\partial^2[P_2](X,T)}{\partial X^2} + \frac{[S_1](X,T)}{\Lambda_1^2(1+([S_1](X,T)/K_1))} + \frac{[S_2](X,T)}{\Lambda_2^2(1+([S_2](X,T)/K_2))} \quad (6)$$

where $[S_1]$, $[S_2]$, and $[P_2]$ are the concentrations of phenol substrate, catechol substrate, and o-quinone product, respectively. $X$ denotes the distance from electrode surface, $\Lambda_1^2$ and $\Lambda_2^2$ are the reaction lengths related to $S_1$ and $S_2$, and

$$\Lambda_1 = \left(\frac{D_f K_1}{k_1[E_T]}\right)^{1/2},\ \Lambda_2 = \left(\frac{D_f K_2}{k_2[E_T]}\right)^{1/2} \quad (7)$$

in which $D_f$ is the diffusion coefficient in the enzyme layer. The other notations have the same meaning as mentioned in nomenclature. $\Lambda_i$ outlines the distance over which $S_i$ can diffuse in the enzyme layer undergoing enzyme reaction. The initial and boundary conditions are [1, 2]:

when $T = 0$, $[S_1] = [S_2] = [P_2] = 0$, and $[S_1](L+\delta, 0) = [S_1]_\infty$ (8)

when $X = 0$, $\frac{\partial[S_1]}{\partial X} = 0, [S_1] + [S_2] = [S_1]_\infty$, and $[P_2] = 0$ (9)

when $X = L + \delta$, $[S_1] = [S_1]_\infty, [S_2] = 0$, and $[P_2] = 0$ (10)

where $L$ is the thickness of the enzymatic layer and $\delta$ is the thickness of the diffusion convection layer. The current density is defined by

$$j_f = -2F\left[\frac{\partial[S_2]}{\partial X}\right]_{X=0} = 2F\left[\frac{\partial[P_2]}{\partial X}\right]_{X=0} \quad (11)$$

The dimensionless form of the nonlinear equations (4)-(6) are given by

$$\frac{\partial u(x,t)}{\partial t} = \frac{\partial^2 u(x,t)}{\partial x^2} - \frac{\mu_1 u(x,t)}{1+\alpha_1 u(x,t)} \quad (12)$$

$$\frac{\partial v(x,t)}{\partial t} = \frac{\partial^2 v(x,t)}{\partial x^2} - \frac{\mu_2 v(x,t)}{1+\alpha_2 v(x,t)} \quad (13)$$

$$\frac{\partial w(x,t)}{\partial t} = \frac{\partial^2 w(x,t)}{\partial x^2} + \frac{\mu_1 u(x,t)}{1+\alpha_1 u(x,t)} + \frac{\mu_2 v(x,t)}{1+\alpha_2 v(x,t)} \quad (14)$$

The corresponding initial and boundary conditions are

when $t = 0, u(x,t) = v(x,t) = w(x,t) = 0,$ and $u(m,0) = 1$ (15)

when $x = 0,\ \frac{\partial u(x,t)}{\partial x} = 0,\ u(x,t) + v(x,t) = 1,$ and $w(x,t) = 0$ (16)

when $x = m, u(x,t) = 1, v(x,t) = 0,$ and $w(x,t) = 0$ (17)

where the dimensionless variables are

$$x = \frac{X}{L}, t = \frac{D_f T}{L^2}, u = \frac{[S_1]}{[S_1]_\infty}, v = \frac{[S_2]}{[S_1]_\infty}, w = \frac{[P_2]}{[S_1]_\infty}, \mu_1 = \frac{L^2}{\Lambda_1^2}, \mu_2 = \frac{L^2}{\Lambda_2^2},\ \alpha_1 = \frac{[S_1]_\infty}{K_1}, \alpha_2 = \frac{[S_1]_\infty}{K_2},$$

$$m = 1 + \frac{\delta}{L} \quad (18)$$

The dimensionless current is

$$I = \frac{j_f}{2F} = -\left(\frac{\partial v(x,t)}{\partial x}\right)_{x=0} \quad (19)$$

where $F$ represents the Faraday constant.

## 3. AN APPROXIMATE ANALYTICAL EXPRESSION OF TRANSIENT CONCENTRATIONS USING HPM

In general, it is challenging to extract exact solutions for nonlinear differential equations that emerge as models of actual physical phenomena. But remarkable advances have been made over the past three decades in finding highly accurate approximate analytical methods. The most common methods include, but are not limited to, Taylor series method [22, 23], variation iteration method (VIM) [24], the series solution technique [25], the residual method [26], Green's function paired along with fixed point theory [27, 28], hyperbolic function and Padé approximation [29], differential transformation method [30], Adomian decomposition method [31] and Akbari-Ganji's method [32, 33].

The homotopy perturbation method (HPM) proposesd by J-H He in 1999 [34] has been one of the most used methods to solve nonlinear systems in diverse fields of science and engineering [35-39]. When we employed the HPM to solve Eqs. (12)-(17), the following approximate analytical expressions for the dimensionless concentrations of substrates and product were obtained (See Appendix A for details):

$$u(x,t) = u_0 \cosh\left(\sqrt{a}x\right) - \frac{\pi}{m^2}\sum_{n=0}^{\infty}\left[\frac{(-1)^n(2n+1)}{(\lambda(n)+\mathrm{a})}\right]\cos\left(\frac{(2n+1)}{2m}\pi x\right)\exp(-(\lambda(n)+a)t) \quad (20)$$

$$v(x,t) = (1-u_0)\left[\begin{array}{c}\dfrac{\sinh\left(\sqrt{b}(m-x)\right)}{\sinh\left(m\sqrt{\mathrm{b}}\right)} \\ +2\pi\sum_{n=0}^{\infty}\left[\dfrac{(-1)^n n}{(n^2\pi^2+m^2\mathrm{b})}\right]\sin\left(\dfrac{n\pi}{m}(m-x)\right)\exp\left(-\left(\dfrac{n^2\pi^2}{m^2}+b\right)t\right)\end{array}\right] \quad (21)$$

$$w(x,t) = f(x,t) - u(x,t) - v(x,t) \quad (22)$$

where

$$f(x,t) = 1 + \frac{2}{\pi}\sum_{n=1}^{\infty}\frac{(-1)^n}{n}\exp\left(-\frac{n^2\pi^2}{m^2}t\right)\left[\sin\left(\frac{n\pi}{m}(m-x)\right) + \sin\left(\frac{n\pi x}{m}\right)\right] \quad (23)$$

$$u_0 = \mathrm{sech}\left(m\sqrt{a}\right), a = \frac{\mu_1}{1+\alpha_1}, b = \frac{\mu_2}{1+\alpha_2(1-u_0)}, \lambda(n) = \frac{(2n+1)^2\pi^2}{4m^2} \quad (24)$$

The current density, from Eq. (11), is given by

$$j_f = \frac{2F[S_1]_\infty(1-u_0)}{L}\left[\sqrt{b}\coth\left(m\sqrt{b}\right) + \frac{2\pi^2}{m}\sum_{n=0}^{\infty}\frac{n^2\exp\left(-\left(\pi^2n^2+b\right)t\right)}{\left(\pi^2n^2+m^2b\right)}\right] \quad (25)$$

and using Eq. (19), the dimensionless current at non steady-state is

$$I = (1-u_0)\left[\sqrt{b}\coth\left(m\sqrt{b}\right) + \frac{2\pi^2}{m}\sum_{n=0}^{\infty}\frac{n^2\exp\left(-\left(\pi^2n^2+b\right)t\right)}{\left(\pi^2n^2+m^2b\right)}\right] \quad (26)$$

### *3.1. Limiting Case: First-Order Kinetics*

Whenever the phenol substrate concentration level in the enzyme layer is significantly lower than the Michaelis constant $K_i$, ($[S_1] << K_i$) or $\alpha_i$ is very small, Eqs. (12)–(14) take on the form:

$$\frac{\partial u(x,t)}{\partial t} = \frac{\partial^2 u(x,t)}{\partial x^2} - \mu_1 u(x,t) \quad (27)$$

$$\frac{\partial v(x,t)}{\partial t} = \frac{\partial^2 v(x,t)}{\partial x^2} - \mu_2 v(x,t) \quad (28)$$

$$\frac{\partial w(x,t)}{\partial t} = \frac{\partial^2 w(x,t)}{\partial x^2} + \mu_1 v(x,t) + \mu_2 v(x,t) \quad (29)$$

The exact solution to the system of Eqs. (27)–(29), subject to boundary conditions Eqs. (15)–(17), can be readily obtained by taking $\alpha_1 = \alpha_2 = 0$ or $a = \mu_1$ and $b = \mu_2$ in Eqs. (20)–(23). Using the same conditions to Eq. (26), the corresponding first-order current can be acquired, from which the expression for bioelectrode sensitivity to phenol substrate and amplification factor can eventually be computed.

### *3.2. Limiting Case: Zero-Order Kinetics*

Whenever the phenol substrate concentration level in the enzyme layer is significantly greater than the Michaelis constant $K_i$, ($[S_1] >> K_i$) or $\alpha_i$ is very large, Eqs. (12)–(14) take on the form:

$$\frac{\partial u(x,t)}{\partial t} = \frac{\partial^2 u(x,t)}{\partial x^2} - \frac{\mu_1}{\alpha_1} \quad (30)$$

$$\frac{\partial v(x,t)}{\partial t} = \frac{\partial^2 v(x,t)}{\partial x^2} - \frac{\mu_2}{\alpha_2} \quad (31)$$

$$\frac{\partial w(x,t)}{\partial t} = \frac{\partial^2 w(x,t)}{\partial x^2} + \frac{\mu_1}{\alpha_1} + \frac{\mu_2}{\alpha_2} \quad (32)$$

The exact solution to the system of Eqs. (30)–(32), subject to boundary conditions Eqs. (15)–(17), can be readily obtained as follows:

$$u(x,t) = 1 + \frac{\mu_1(X^2-m^2)}{2\alpha_1} + \frac{16\mu_1 m^2}{\alpha_1\pi^3}\sum_{n=1}^{\infty}\frac{(-1)^n}{(2n-1)^3}\exp\left(-\frac{(2n-1)^2\pi^2}{4m^2}t\right)\cos\left(\frac{(2n-1)\pi x}{2m}\right) \quad (33)$$

$$v(x,t) = f(x,t) - u(x,t) - w(x,t) \quad (34)$$

$$w(x,t) = -\left(\frac{\alpha_1\mu_2+\alpha_2\mu_1}{\alpha_1\alpha_2}\right)\frac{2m^2}{\pi^3}\sum_{n=1}^{\infty}\frac{(-1)^n}{n^3}\left\{1-\exp\left(-\frac{n^2\pi^2}{m^2}t\right)\right\}\left[\sin\left(\frac{n\pi x}{m}\right)+\sin\left(\frac{n\pi(m-x)}{m}\right)\right] \quad (35)$$

where $f(x,t)$ is defined in Eq. (23).

The dimensionless current is given by

$$I = \left(\frac{\alpha_1\mu_2+\alpha_2\mu_1}{\alpha_1\alpha_2}\right)\frac{2m}{\pi^3}\sum_{n=1}^{\infty}\frac{[1+(-1)^{n+1}]}{n^2}\left\{1-\exp\left(-\frac{n^2\pi^2}{m^2}t\right)\right\} \quad (36)$$

## 4. AN APPROXIMATE ANALYTICAL EXPRESSION OF STEADY-STATE CONCENTRATIONS USING AGM

The Akbari-Ganji method (AGM), which was first put forth by M. Akbari and D. Ganji [40], has been successfully applied to find analytical solutions of nonlinear systems [41]. Berkan et al. [42] investigated the 3D problem of condensation film on inclined rotating disk electrodes analytically using AGM. Derakhshan et al. [43] used AGM to discuss the process of heat and mass transfer in steady nanofluid flow between two parallel plates in the existence of a uniform magnetic field. Mary et al. [44] employed the AGM to solve a nonlinear reaction-diffusion equation in an immobilized enzymes system.

In this paper, AGM is applied to determine the approximate analytical solution of steady-state nonlinear equations. Using this method, the derived steady-state concentrations of substrates and product are, respectively, given by (see Appendix C).

$$u_{ss}(x) = u_0 \cosh\left(\sqrt{a}x\right) \tag{37}$$

$$v_{ss}(x) = \frac{(1-u_0)\sinh\left(\sqrt{b}(m-x)\right)}{\sinh\left(m\sqrt{b}\right)} \tag{38}$$

$$w_{ss}(x) = 1 - u_0 \cosh\left(\sqrt{a}x\right) - \frac{(1-u_0)\sinh\left(\sqrt{b}(m-x)\right)}{\sinh\left(m\sqrt{b}\right)} \tag{39}$$

Interestingly, as $t \to \infty$, the analytical expressions obtained in Eqs. (20)–(22) by HPM are reduced exactly to the Eqs. (37)–(39).

Now form Eq. (11), the current density takes on the form

$$J_{\mathrm{f}} = \frac{2F[S_1]_\infty}{L}\sqrt{b}(1-u_0)\ \coth\left(m\sqrt{b}\right) \tag{40}$$

and the dimensionless current at steady-state is

$$I_{\mathrm{ss}} = \sqrt{b}(1-u_0)\ \coth\left(m\sqrt{b}\right) \tag{41}$$

Moreover, the sensitivity $S_{ph}$ of the bioelectrode toward phenol substrate [20] is given by

$$S_{ph} = -\frac{J_f}{[S_1]_\infty} = -\frac{2F}{L}\sqrt{b}(1-u_0)\ \coth\left(m\sqrt{b}\right) \tag{42}$$

and the amplification factor can be obtained as follows:

$$\mathrm{AF} = m\sqrt{b}\ \coth\left(m\sqrt{b}\right) \tag{43}$$

## 5. RESULTS AND DISCUSSION

Equations (20)–(22) are the derived analytical expressions for the concentrations of phenol substrate $u$, catechol substrate $v$, and o-quinone product $w$ assuming transient conditions, while Eqs. (37)–(39) are the new simple analytical expressions of concentrations for the steady-state case.

### *5.1. Validation of Analytical Results*

The derived results are found to agree substantially with the numerical results generated by MATLAB simulations. For example, Figure 2 (non-steady-state) and Table 1 (steady-state) show that

the derived analytical results are very close to the numerical results representing the concentrations of phenol substrate, catechol substrate, and o-quinone product. Table 2 shows a satisfactory agreement between the approximate analytical substrates and product concentrations with the exact limiting case results (first-order kinetics).

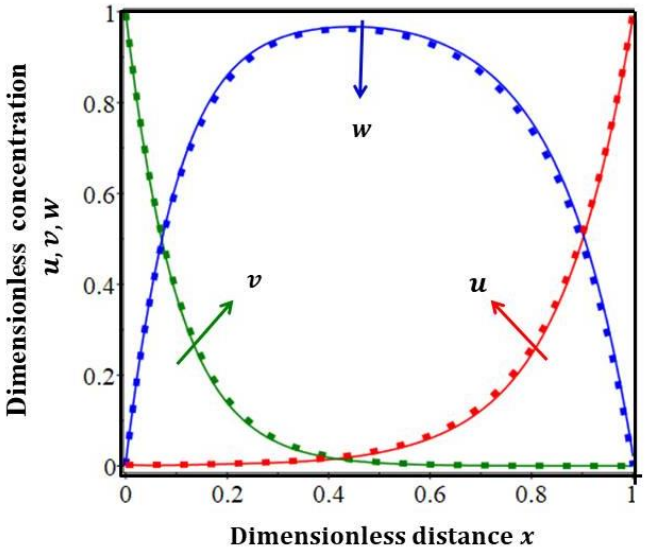


**Figure 2.** Comparison between analytical (solid lines) and numerical (dotted lines) results.

The analytical curves represent the concentration of phenol substrate $u$ (Eq. (20)), catechol substrate $v$ (Eq. (21)), and o-quinone product $w$ (Eq. (22)). The parameters used are $\mu_1 = 50,\ \alpha_1 = 0.1, \mu_2 = 100,\ \alpha_2 = 0.1,\ m = 1,$ and $t = 10$, as in ref. [21].

Figure 2 shows the normalized concentration profile of substrates and product. It shows that the concentration of catechol substrate is increasing, the concentration of phenol substrate is decreasing function from the interface of the solution to the electrode. At the same time, the o-quinone product curves attain a maximum value at $x = 0.4357$, halfway from the electrode surface.

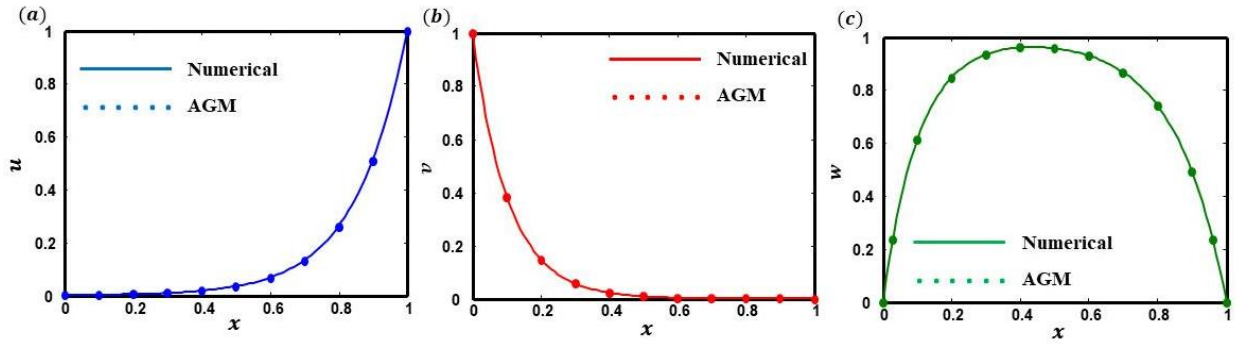


**Figure 3.** Plot of the dimensionless concentrations of $(a)$ phenol substrate $(b)$ catechol substrate $(c)$ o-quinone product at steady-state. The parameters used are $\mu_1 = 50,\ \alpha_1 = 0.1,\ \mu_2 = 100,\ \alpha_2 = 0.1,$ and $m = 1$.

The accuracy of the proposed analytical AGM approximations is portrayed in Figure 3, where the approximate analytical expressions show strong agreement with the numerical results obtained through fourth-order Runge-Kutta method.

*5.2. Influence of Various Parameters on Current and Sensitivity*

The accuracy of the proposed analytical AGM approximations is portrayed in Figure 3, where the approximate analytical concentrations of phenol substrate ($u$), catechol substrate ($v$), and o-quinone product ($w$) show strong agreement with the numerical results obtained by the numerical fourth-order Runge-Kutta method.

**Table 1.** Comparison of analytical results of concentration of phenol substrate $u$, catechol substrate $v$ and o-quinone product $w$ for steady-state with numerical results (Num.) for the values $\mu_1 = 50, \mu_2 = 100, \alpha_1 = 0.01, \alpha_2 = 0.1, m = 1$ [21].

| $x$ | **Concentration of phenol substrate $u$** | | **Concentration of catechol substrate $v$** | | **Concentration of o-quinone product $w$** | |
|---|---|---|---|---|---|---|
| | **Num.** | **Analytic Eq. (37)** | **Num.** | **Analytic Eq. (38)** | **Num.** | **Analytic Eq. (39)** |
| 0 | 0.0017 | 0.0018 | 0.9983 | 0.9982 | 0 | 0 |
| 0.2 | 0.0037 | 0.0038 | 0.1390 | 0.1483 | 0.8573 | 0.8479 |
| 0.4 | 0.0145 | 0.0147 | 0.0189 | 0.0220 | 0.9666 | 0.9633 |
| 0.6 | 0.0593 | 0.0600 | 0.0026 | 0.0033 | 0.9381 | 0.9368 |
| 0.8 | 0.2437 | 0.2448 | 0.0003 | 0.0005 | 0.7560 | 0.7547 |
| 1 | 1 | 1 | 0 | 0 | 0 | 0 |

**Table 2.** Comparison between approximate analytical results and exact results for the limiting case for the dimensionless concentration of phenol substrate, catechol substrate, and o-quinone product given the parameters $\mu_1 = 50,\ \alpha_1 = 0.1, m = 1,\ \mu_2 = 100,\ \alpha_2 = 0.1$ and $t = 10$.

| $x$ | **Concentration of phenol substrate $(u)$** | | **Concentration of catechol substrate $(v)$** | | **Concentration of o-quinone product $(w)$** | |
|---|---|---|---|---|---|---|
| | **Analytic Eq. (20)** | **Limiting case** | **Analytic Eq. (21)** | **Limiting case** | **Analytic Eq. (22)** | **Limiting case** |
| 0 | 0.0024 | 0.0017 | 0.9976 | 0.9983 | 0 | 0 |
| 0.2 | 0.0049 | 0.0037 | 0.1482 | 0.1351 | 0.8469 | 0.8612 |
| 0.4 | 0.0176 | 0.0144 | 0.022 | 0.0183 | 0.9604 | 0.9673 |
| 0.6 | 0.0674 | 0.0591 | 0.0033 | 0.0025 | 0.9293 | 0.9384 |
| 0.8 | 0.2597 | 0.2431 | 0.0005 | 0.0003 | 0.7398 | 0.7566 |
| 1 | 1 | 1 | 0 | 0 | 0 | 0 |

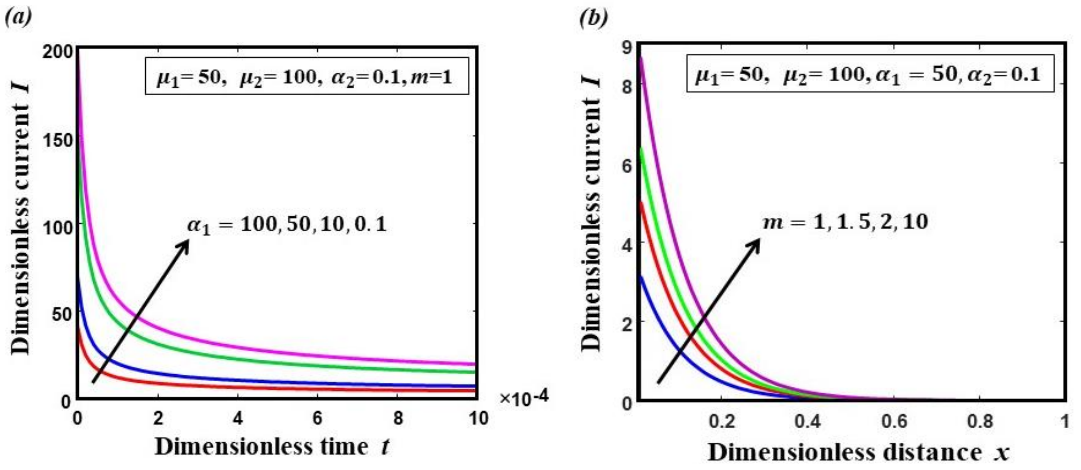


**Figure 4.** Graph of dimensionless current vs. $(a)$ the dimensionless time for different values of $\alpha_1$ $(b)$ the dimensionless distance $x$ for different values of $m$.

**Table 3.** Computed dimensionless transient current $(I)$ for various values of the dimensionless parameters $t$ and $\alpha_2$ for the fixed parameters values $\mu_1 = 50, \alpha_1 = 0.1,\ \mu_2 = 100,$ and $m = 1$.

| | **Dimensionless Current $I$** | | | | | |
|---|---|---|---|---|---|---|
| $\alpha_2$ | $t = 10^{-3}$ | $t = 10^{-2}$ | $t = 10^{-1}$ | $t = 10^{0}$ | $t = 10^{1}$ | $t = 10^{2}$ |
| 0.01 | 19.5329 | 10.4362 | 9.9270 | 9.9270 | 9.9270 | 9.9270 |
| 0.1 | 19.3935 | 10.092 | 9.5131 | 9.5131 | 9.5131 | 9.5131 |
| 1 | 18.6828 | 8.2327 | 7.0595 | 7.0586 | 7.0586 | 7.0586 |
| 10 | 17.9610 | 6.1337 | 3.1938 | 3.0257 | 3.0257 | 3.0257 |
| 100 | 17.8168 | 5.6843 | 1.9538 | 1.3077 | 1.3077 | 1.3077 |
| 1000 | 17.8009 | 5.6342 | 1.7979 | 1.0308 | 1.0307 | 1.0307 |
| 10000 | 17.7993 | 5.6291 | 1.7819 | 1.0011 | 1.0010 | 1.0010 |

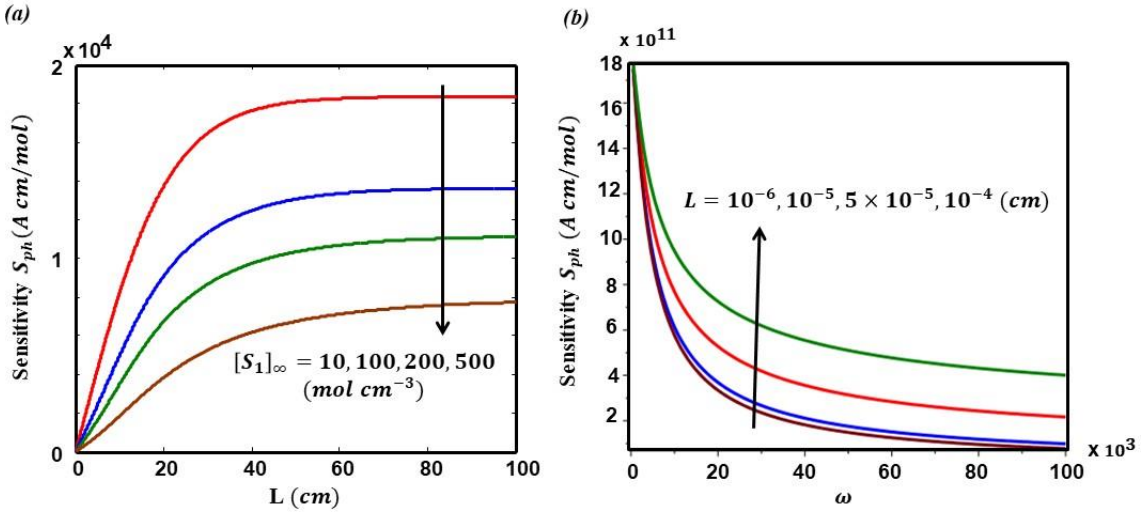


**Figure 5.** Plot of sensitivity $(S_{\text{ph}})$ for the parameters given in Table 4 $(a)$ against $L$ for various experimental values of parameter $[S_1]_\infty$ $(b)$ against $\omega$ for various values of parameter $L$.

**Table 4.** Values of the parameters used in Figure 5.

| Parameter | Figure 5(a) | Figure 5(b) |
|---|---|---|
| $K_1$ | 100 mol cm$^{-3}$ | $2.8 \times 10^{-7}$ mol cm$^{-3}$ |
| $K_2$ | 100 mol cm$^{-3}$ | $2.5 \times 10^{-7}$ mol cm$^{-3}$ |
| $\Lambda_1$ | 10 cm | $1.19 \times 10^{-7}$ cm |
| $\Lambda_2$ | 10 cm | $1.07 \times 10^{-7}$ cm |
| $D_e$ | $1.5 \times 10^{-6}$ cm$^2$ s$^{-1}$ | $2.2 \times 10^{-5}$ cm$^2$ s$^{-1}$ |
| $\nu$ | 0.01 cm$^2$ s$^{-1}$ | 0.01 cm$^2$ s$^{-1}$ |
| $[S_1]_\infty$ | - | 1 mol cm$^{-3}$ |
| $\omega$ | 20 rpm | - |

The fact that the bioelectrode is highly sensitive to smaller bulk concentrations of phenol substrate is confirmed in Figure 5(a). It is also interesting to note that the sensitivity curves become linear as the enzymatic layer thickness increases. The stable value of $S_{\text{ph}}$, thus, reaches $\frac{2F}{\Lambda_2\sqrt{1+\alpha_2}}$. Sensitivity to minimal bulk concentrations of phenol substrate makes it critical to keep track of the system's sensitivity for the first-order kinetics, as seen in Figure 5(b). It is observed in Figure 5(b) that phenol sensitivity reaches high value for slow rotations of the bioelectrode. In general, thick enzymatic layer contributes to good phenol sensitivity.

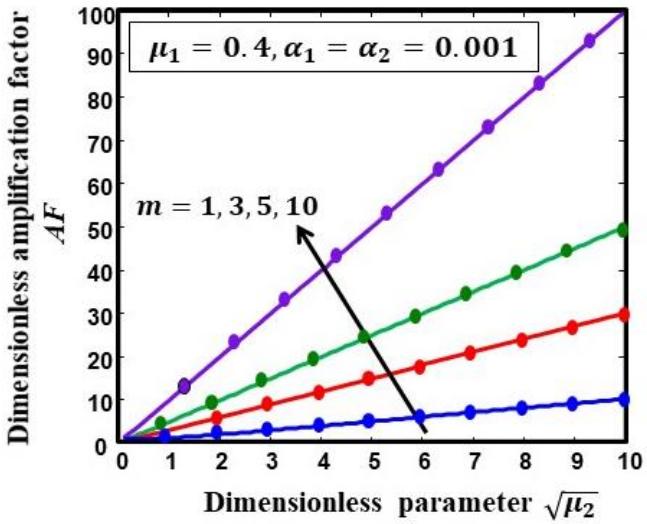


**Figure 6.** Plot of amplification factor against the dimensionless parameter $(\sqrt{\mu_2})$ for various values of $m$. The solid line is the derived result in Eq. (36), which is shown to coincide with the dotted curve representing Eq. (43) in [21].

As shown in Figure 6, the amplification factor rises with higher enzyme activity $\sqrt{\mu_2}$. Since the parameter $m$ is influenced by the ratio $\delta/L$, then bioelectrodes with higher $m$ values or thicker

convection-diffusion layer $\delta$ are more amplified. It can further be inferred from $\delta = \frac{1.61\sqrt[3]{D_e}\sqrt[6]{v}}{\sqrt{\omega}}$ [20] that lower rotation rates spike the amplification factor.

### *5.3. Differential Sensitive Analysis of Parameters*

The partial derivative of the current with respect to a parameter determines the effect of that parameter on the current [45]. Figure 7 shows that the percentages of change in current with respect to $\Lambda_2, [S_1]_\infty, K_1, L, \delta, K_2, \Lambda_1$ are 38%, 19%, 18%, 11%, 7%, 6% and 1%, respectively. Therefore, the reaction lengths related to $S_2$, that is $\Lambda_2$ has the highest influence on the current, while $\Lambda_1$ has least influence on the current.

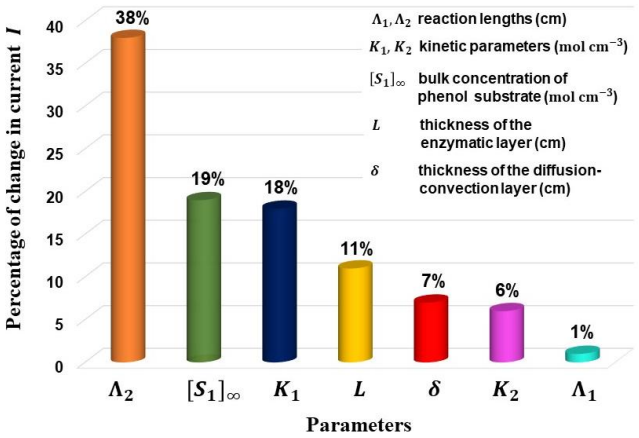


**Figure 7.** Influence of various parameters on steady-state current.

## 6. CONCLUSION

This paper presented two closed-form analytical solutions for the coupled transient nonlinear reaction-diffusion equations, modeling amperometric biosensor's transient responses. Approximate analytical expressions for the transient and stationary concentration of phenol, catechol substrate, and o-quinone product have been derived. These derived approximate analytic results concurred with MATLAB-generated numerical results. In addition, a study on the effects of the governing system's parameters on the current, sensitivity, and amplification factor has been presented. The results of this study can be utilized to determine the biosensor's kinetic characteristics. Moreover, the simplicity and reliability of the proposed approaches, as well as their accessibility, would make them usable for determining the approximate amounts of substrate and product concentrations and current for reciprocal competitive inhibition.

DECLARATION OF COMPETING INTEREST

The authors declare that they have no known competing financial interests or personal relationships that could have appeared to influence the work reported in this paper.

ACKNOWLEDGEMENT

The authors are grateful to Shri J. Ramachandran, Chancellor, Col. Dr. G. Thiruvasagam, Vice-Chancellor and Dr. M. Jayaprakashvel, Registrar, Academy of Maritime Education and Training (AMET), Chennai, Tamil Nadu for their encouragement. They are also thankful to the reviewers for their comments.

## APPENDIX A. OBTAINING THE APPROXIMATE ANALYTICAL SOLUTION OF EQ. (12) USING HPM

The homotopy for Eq. (12) is constructed as follows [34]:

$$(1-p)\left[\frac{\partial u(x,t)}{\partial t}-\frac{\partial^2 u(x,t)}{\partial x^2}+\frac{\mu_1 u(x,t)}{1+\alpha_1 u(m,0)}\right]+p\left[\frac{\partial u(x,t)}{\partial t}-\frac{\partial^2 u(x,t)}{\partial x^2}+\frac{\mu_1 u(x,t)}{1+\alpha_1 u(x,t)}\right]=0, \quad \text{(A.1)}$$

and by applying the initial condition in Eq. (14) we get,

$$(1-p)\left[\frac{\partial u(x,t)}{\partial t}-\frac{\partial^2 u(x,t)}{\partial x^2}+\frac{\mu_1 u(x,t)}{1+\alpha_1}\right]+p\left[\frac{\partial u(x,t)}{\partial t}-\frac{\partial^2 u(x,t)}{\partial x^2}+\frac{\mu_1 u(x,t)}{1+\alpha_1 u(x,t)}\right]=0. \quad \text{(A.2)}$$

We search for an approximate solution of Eq. (A.2) of the form

$$u(x,t)=u_0(x,t)+pu_1(x,t)+p^2u_2(x,t)+\cdots. \quad \text{(A.3)}$$

Substituting Eq. (A.4) into Eq. (A.2) and equating the coefficients of zeroth power of $p$ gives:

$$\frac{\partial u_0(x,t)}{\partial t}-\frac{\partial^2 u_0(x,t)}{\partial x^2}+Au_0(x,t)=0, \quad \text{(A.4)}$$

where $=\frac{\mu_1}{1+\alpha_1}$ , and subject to the initial and boundary conditions given in Eq. (14). In Laplace plane, we express Eq. (A.4) in the form

$$\frac{d^2\overline{u_0}(x,s)}{dx^2}-(s+A)\overline{u_0}(x,s)=0, \quad \text{(A.5)}$$

with boundary conditions

$$\text{At } x=0, \frac{\partial\overline{u_0}(x,s)}{\partial x}=0, \text{ At } x=m, \overline{u_0}(x,s)=\frac{1}{s}, \quad \text{(A.6)}$$

where $\overline{u_0}(x,s)$ represents the Laplace transformation of $u_0(x,t)$. The solution of system (A.5)–(A.6) is given by

$$\overline{u_0}(x,s)=\frac{\cosh\left(\sqrt{s+A}x\right)}{s\cosh\left(m\sqrt{s+A}\right)}. \quad \text{(A. 7)}$$

To deduce $u_0(x,t)$, we use the following complex inversion formula

$$u_0(x,t)=\frac{1}{2\pi i}\int_{\gamma-i\infty}^{\gamma+i\infty}e^{sT}\,\overline{u_0}(x,s)ds. \quad \text{(A.8)}$$

To proceed, we need to determine the residue of $\overline{u_0}(x,s)$, that is

$$\text{Res}\left[\frac{\cosh\left(\sqrt{s+A}x\right)}{s\cosh\left(m\sqrt{s+A}\right)}\right]. \quad \text{(A.9)}$$

At $s = 0$, we obtain a simple pole and the solution of $\cosh\left(m\sqrt{s+A}\right) = 0$ generates infinitely many poles given by $s_n = -\frac{(2n+1)^2\pi^2}{4m^2} - A$, where $n = 0, 1, 2, \cdots$. Hence

$$\text{Res}\left[\frac{\cosh\left(\sqrt{s+A}x\right)}{s\cosh\left(m\sqrt{s+A}\right)}\right] = \left[\frac{\cosh\left(\sqrt{s+A}x\right)}{s\cosh\left(m\sqrt{s+A}\right)}\right]_{s=0} + \text{Res}\left[\frac{\cosh\left(\sqrt{s+A}x\right)}{s\cosh\left(m\sqrt{s+A}\right)}\right]_{s=s_n}. \quad \text{(A.10)}$$

The residue at $s = 0$ is given by

$$\text{Res}\left[\frac{\cosh\left(\sqrt{s+A}x\right)}{s\cosh\left(m\sqrt{s+A}\right)}\right]_{s=0} = \lim_{s\to 0}\left[\frac{(s-0)e^{st}\cosh\left(\sqrt{s+A}x\right)}{s\cosh\left(m\sqrt{s+A}\right)}\right] = \frac{\cosh\left(\sqrt{A}x\right)}{\cosh\left(m\sqrt{A}\right)}, \quad \text{(A.11)}$$

and the residue at $s = s_n$ is given by

$$\text{Res}\left[\frac{\cosh\left(\sqrt{s+A}x\right)}{s\cosh\left(m\sqrt{s+A}\right)}\right]_{s=s_n} = \lim_{s\to s_n}\left[\frac{e^{st}}{s}\frac{\cosh\left(\sqrt{s+A}x\right)}{\frac{d}{ds}\cosh\left(m\sqrt{s+A}\right)}\right]$$

$$= -\frac{\pi}{m}\sum_{n=0}^{\infty}\frac{(2n+1)e^{-\left(\frac{(2n+1)^2\pi^2}{4m^2}+A\right)t}\cos\left(\frac{(2n+1)\pi x}{2m}\right)}{\left[\frac{(2n+1)^2\pi^2}{4m^2}+A\right]\sin\left(\frac{(2n+1)\pi}{2m}\right)}. \quad \text{(A.12)}$$

From Eqs. (A.8)–(A.11), we get the concentration of substrate $u(x,t) \approx u_0(x,t)$, which is the result given by Eq. (20) in the text. Similarly, we can derive Eq. (13).

## APPENDIX B. RELATIONSHIP BETWEEN $u(x,t)$ , $v(x,t)$ AND $w(x,t)$

Introduce a function $f(x,t) = u(x,t) + v(x,t) + w(x,t)$, so that Eqs. (12)–(14) satisfy

$$\frac{\partial f(x,t)}{\partial t} = \frac{\partial^2 f(x,t)}{\partial x^2}, \quad \text{(B.1)}$$

subject to the initial and boundary conditions given by

$$f(x,0) = 0,\ f(0,t) = 1,\ \text{and}\ f(m,t) = 1. \quad \text{(B.2)}$$

Equations (B.1) and (B.2) take the following form in the Laplace plane:

$$\frac{d^2\bar{f}(x,s)}{dx^2} - s\bar{f}(x,s) = 0 \quad \text{(B.3)}$$

$$\bar{f}(0,s) = \bar{f}(m,s) = \frac{1}{s}. \quad \text{(B.4)}$$

The solution of system (B.3)-(B.4) is

$$\bar{f}(x,s) = \frac{\sinh\left(\sqrt{s}(m-x)\right)}{s\sinh\left(m\sqrt{s}\right)} + \frac{\sinh\left(\sqrt{s}x\right)}{s\sinh\left(m\sqrt{s}\right)}. \quad \text{(B.5)}$$

When we take the inverse Laplace transform to Eq. (B.5), we get

$$f(x,t) = 1 + \frac{2}{\pi}\sum_{n=1}^{\infty}\frac{(-1)^n}{n}\exp\left(-\frac{n^2\pi^2}{m^2}t\right)\left[\sin\left(\frac{n\pi}{m}(m-x)\right) + \sin\left(\frac{n\pi x}{m}\right)\right] \quad \text{(B.6)}$$

## APPENDIX C. OBTAINING THE APPROXIMATE ANALYTICAL SOLUTION ((12)-(14)) USING AGM

The dimensionless form of the nonlinear differential equations (12)–(14) for Michaelis–Menten formalism at steady-state is as follows:

$$\frac{d^2u(x)}{dx^2} - \frac{\mu_1 u(x)}{1+\alpha_1 u(x)} = 0, \tag{C.1}$$

$$\frac{d^2v(x)}{dx^2} - \frac{\mu_2 v(x)}{1+\alpha_2 v(x)} = 0, \tag{C.2}$$

$$\frac{d^2w(x)}{dx^2} + \frac{\mu_1 u(x)}{1+\alpha_1 u(x)} + \frac{\mu_2 v(x)}{1+\alpha_2 v(x)} = 0, \tag{C.3}$$

and the corresponding boundary conditions are

$$\text{for } x = 0\text{: } \frac{du(x)}{dx} = 0,\ u(x) + v(x) = 1, \text{and } w(x) = 0, \tag{C.4}$$

$$\text{for } x = m, u(x) = 1, v(x) = 0, \text{and } w(x) = 0. \tag{C.5}$$

The approximate analytical solutions for Eqs. (C.1) and (C.2) is assumed to be in the form:

$$u(x) = A_1 \cosh(lx) + B_1 \sinh(lx), \tag{C.6}$$

$$v(x) = A_2 \cosh(nx) + B_2 \sinh(nx). \tag{C.7}$$

Using the boundary conditions (C.4) and (C.5), we obtain the following values:

$$A_1 = u_0,\ B_1 = 0,\ A_2 = 1 - u_0, B_2 = \coth(mn)(u_0 - 1),\ u_0 = \operatorname{sech}(ml) \tag{C.8}$$

Substituting these values into (C.6) and (C.7) and then into Eqs. (C.1) & (C.2), we get

$$\frac{l^2 \cosh(lx)}{\cosh(mx)} - \frac{\mu_1 \cosh(lx)}{\alpha_1 \cosh(lx) + \cosh(mx)} = 0, \tag{C.9}$$

$$A_2 n^2 \cosh(nx) + B_2 n^2 \sinh(nx) - \frac{\mu_2 (A_2 \cosh(nx) + B_2 \sinh(nx))}{\alpha_2 (A_2 \cosh(nx) + B_2 \sinh(nx)) + 1} = 0. \tag{C.10}$$

By substituting $x = m$ into Eq. (C.9) and $x = 0$ in Eq. (C.10), we have

$$l = \sqrt{\frac{\mu_1}{1+\alpha_1}}, n = \sqrt{\frac{\mu_2}{1+\alpha_2 - \alpha_2 \operatorname{sech}(ml)}}. \tag{C.11}$$

Adding Eqs. (C.1)–(C.3), we get

$$\frac{d^2[u(x)+v(x)+w(x)]}{dx^2} = 0, \tag{C.12}$$

subject to the boundary condition

$$\text{when } x = 0,\ u(x) + v(x) + w(x) = 1, \tag{C.13}$$

$$\text{when } x = m, u(x) + v(x) + w(x) = 1. \tag{C.14}$$

By letting $u(x) + v(x) + w(x) = f(x)$, Eq. (C.13) becomes

$$\frac{d^2 f(x)}{dx^2} = 0, \tag{C.15}$$

for which the boundary conditions are reduced to

$f(0) = 1$ and $f(m) = 1.$ (C.16)

The solution of Eqs. (C.15)–(C.16) is clearly $f(x) = 1$, and hence

$w(x) = 1 - u(x) - v(x).$ (C.17)

## References


1. I.E. Tothill, A.P.F. Turner, Encyclopedia of Food Sciences and Nutrition, (Second Edition), Academic Press, (2003) London, UK.
2. J. Richard Aspland, Marie-Claire Hennion, Techniques and Instrumentation in Analytical Chemistry, (1997) Elsevier, Amsterdam, Netherlands.
3. M. Teresa Fernández Abedul, Laboratory Methods in Dynamic Electroanalysis, (2020) Elsevier, Amsterdam, Netherlands.
4. L. Zhang, Y. Zhang, L. Ma, F. Ren, Y. Sun, X. Sun, *AIP Conf Proc*., 2073 (2019) 020042.
5. S. Pasika, S. T. Gandla, Heliyon, 6(7) (2020) e04096.
6. R. Preuss, H. M. Koch, J. Angerer, *J. Chromatogr. B*., 816 (2005) 269.
7. S. Uchiyama, Y. Hasebe, H. Shimizu, H. Ishihara, *Anal. Chim. Acta*., 276 (1993) 341.
8. Y. Hasebe, Y. Tanaka, S. Uchiyama, *Anal. Lett*., 27 (1994) 41.
9. C.G. Bauer, A.V. Eremenko, E. Ehrentreich-Forster, F.F. Bier, A. Makower, H.B. Halsall, W.R. Heineman, F.W. Scheller, *Anal. Chem*., 68 (1996) 2453.
10. X. Tang, G. Johansson, *Anal. Lett*., 28 (1995) 2595.
11. J.-L. Besombes, S. Cosnier, P. Labbe´, G. Reverdy, *Anal. Lett*., 28 (1995) 405.
12. E. Burestedt, A. Narvaez, T. Ruzgas, L. Gorton, J. Emmneus, E.Dominguez, G. Marko Varga, *Anal. Chem*., 68 (1996) 1605.
13. T.J. Moore, M.J. Joseph, B.W. Allen, L.A. Coury, *Anal. Chem*., 67 (1995) 1896.
14. V. Desprez, P. Labbé, *J. Electroanal. Chem*., 415 (1996) 191.
15. P.N. Bartlett, R.G. Whitaker, *J. Electroanal. Chem*. *Interf. Electrochem.,* 224 (1987) 27.
16. S. Cosnier, J.-J. Fombon, P. Labbé, D. Limosin, *Sens. Actuators B Chem*. 59 (1999) 134.
17. D. Shan, S. Cosnier, C. Mousty, Anal. Chem., 75 (2003) 3872.
18. P. O¨nnerfjord, J. Emne´us, G. Marko-Varga, L. Gorton, F. Ortega and E. Dominguez, *Biosensors Bioclectron*., 10 (1995) 607.
19. J.-L. Besombes, S. Cosnier, P. Labbe, G. Reverdy, *Anal. Lett*., 28 (1995) 405.
20. L. Coche-Guerente, P. Labbé, V. Mengeaud, *Anal. Chem*., 73 (2001) 3206.
21. K. Indira, L. Rajendran, *Electrochim. Acta*, 56 (2011) 6411.
22. S. Vinolyn Sylvia, R. Joy Salomi, L. Rajendran, M Abukhaled, *Solid State Technol*., 63 (2020) 10090.
23. S. Vinolyn Sylvia, R. Joy Salomi, L. Rajendran, Marwan Abukhaled, *J. Math. Chem*., 59 (2021).
24. A.M. Wazwaz, *Optik*, 207 (2020) 164457.
25. R. Joy Salomi, S. Vinolyn Sylvia, L. Rajendran, M. Abukhaled, *Sens. Actuators B Chem*., 321 (2020) 128576.
26. K. Saranya, V. Mohan, L. Rajendran, *J. Math. Chem*., 58 (2020) 1230.
27. M. Abukhaled, S.A. Khuri, *Int. J. Appl. Math*. *Comput. Sci*., 7 (2021) 1.
28. M. Abukhaled, S.A. Khuri, *Math. Comput. Appl*., 24 (2019) 8.
29. J. Visuvasam, A. Meena, L. Rajendran*, J. Electroanal. Chem*., 869 (2020) 114106.
30. M. Chitra Devi, P. Pirabaharan, L. Rajendran, M. Abukhaled, *React. Kinet. Mech. Catal*., 133 (2021) 655.
31. R. Rach, J.S. Duan, A.M. Wazwaz, *Int. J. Dyn. Syst. Differ. Equ*., 10 (2020) 287.
32. M.E.G. Lyons*, Int. J. Electrochem. Sci*., 4 (2009) 1196.
33. M.E.G. Lyons, *J. Electroanal. Chem*., 872 (2020) 114278.

34. J.H. He, *Comput Methods Appl Mech Eng*., 178 (1999) 257.
35. J.H. He, Internat. *J. Non-Linear Mech*., 35 (2000) 37.
36. L. Rajendran, R. Swaminathan, K. Venugopal, M. Rasi, M. Abukhaled, *Quim. Nova*, 43 (2020) 58.
37. S. Vinolyn Sylvia, R. Joy Salomi, M.E.G. Lyons, L. Rajendran, *Int. J. Electrochem. Sci*., 16 (2021) 1.
38. R. Joy Salomi, S. Vinolyn Sylvia, M.E.G. Lyons, L. Rajendran, *J. Electroanal. Chem*. 895 (2021) 115421.
39. S. Saravanakumar, A. Eswari, L. Rajendran, M. Abukhaled, *Appl. Math. Inf. Sci*., 14 (2020) 967.
40. M.R. Akbari, D.D. Ganji, M. Nimafar, A.R. Ahmadi, *Front. Mech. Eng*., 9 (2014) 390. Dharmalingam, M. Veeramuni, *J. Electroanal. Chem*., 844 (2019) 1.
41. S. Berkan, S.R. Hoseini, D.D. Ganji, *Populs. Power Res*., 6 (2017) 277.
42. R. Derakhshan, A. Shojaei, K. Hosseinzadeh, M. Nimafar, D.D. Ganji, *Case Stud. Therm. Eng*., 14 (2019) 100439.
43. M.L.C. Mary, M.C. Devi, A. Meena, L. Rajendran, M. Abukhaled, *Reac. Kinet. Mech. Cat*., 134 (2021) 641.
44. M. Rasi, L. Rajendran, A. Subbiah, *Sens. Actuators B Chem*., 208 (2015) 128.